"NOTICE: When Government or other drawings, specifications or other data are used for any purpose other than in connection with a definitely related Government procurement operation, the U.S. Government thereby incurs no responsibility, nor any obligation whatsoever; and the fact that the Government may have formulated furnished, or in any way supplied the said drawings, specifications or other data is not to be regarded by implication or otherwise as in any manner licensing the holder or any other person or corporation, or conveying any rights or permission to manufacture, use or sell any patented invention that may in any way be related thereto

WADC TECHNICAL REPORT 59-87
PART II

DETERMINATION OF FACTORS GOVERNING SELECTION AND APPLICATION OF MATERIALS FOR ABLATION COOLING OF HYPERVELOCITY VEHICLES

John H. Bonin
Channon F. Price
Donald E. Taylor

Chicago Midway Laboratories
The University of Chicago

JULY 1959

WRIGHT AIR DEVELOPMENT CENTER

WADC TECHNICAL REPORT 59-87
PART II

DETERMINATION OF FACTORS GOVERNING SELECTION AND APPLICATION OF MATERIALS FOR ABLATION COOLING OF HYPERVELOCITY VEHICLES

John H. Bonin
Channon F. Price
Donald E. Taylor

Chicago Midway Laboratories
The University of Chicago

JULY 1959

Materials Laboratory
Contract No. AF 33 (616)-5436
Project No. 7360

WRIGHT AIR DEVELOPMENT CENTER
AIR RESEARCH AND DEVELOPMENT COMMAND
UNITED STATES AIR FORCE
WRIGHT-PATTERSON AIR FORCE BASE, OHIO

500 – September 1959 – 3-84

FOREWORD

This is the second part of a report prepared by the Chicago Midway Laboratories of The University of Chicago under USAF Contract No. AF 33(616)-5436. This contract was initiated under Project 7360, "Materials Analysis and Evaluation Techniques," Task No. 73603, "Thermodynamics and Heat Transfer." It was administered under the direction of the Materials Laboratory, Directorate of Laboratories, Wright Air Development Center, with Mr. Hyman Marcus acting as project engineer.

This part of the report covers sample testing results on a series of twenty-two samples tested under a supplementary agreement to the above contract. The samples were tested in May, July, and September, 1958.

Chicago Midway Laboratories personnel who participated in the work reported in this phase include Messrs. J. H. Bonin, C. F. Price, and Edward Yelke.

Chicago Midway Laboratories wishes to acknowledge the help and suggestions of Messrs. H. Marcus, R. E. Otto, D. Schmidt, G. Sonnenschein, and J. I. Wittebort of the Materials Laboratory, Wright Air Development Center.

ABSTRACT

The results obtained from tests of samples of twenty-two different materials are presented. The samples were exposed to the high-temperature plasma discharge produced in an air-stabilized electric arc. The sample shape, test conditions and test procedure, and the material behavior are reported upon.

PUBLICATION REVIEW

This report has been reviewed and is approved.

FOR THE COMMANDER:

LEO F. SALZBERG
Chief, Materials Physics Branch
Materials Laboratory

TABLE OF CONTENTS

		Page
1.	Introduction	1
2.	Test Description	1
	2.1 Operating Conditions and Sample Position	1
	2.2 Sample Shape	1
	2.3 Test Procedure	1
	2.4 Materials Tested	2
3.	Test Results	2
4.	General Remarks	9
APPENDIX I:	Sample Photographs, Silhouettes, and Test Remarks	11

LIST OF ILLUSTRATIONS

Figure		Page
1	Standard sample shape.	3
2	Stagnation point ablation as a function of time for samples as noted	6
3	Stagnation point ablation as a function of time for sample Nos. Y-5 and Y-6	7
4	Stagnation point ablation as a function of time for sample Nos. Y-7 and Y-8	7
5	Stagnation point ablation as a function of time for sample Nos. Y-17 and Y-19	7
6	Stagnation point ablation as a function of time for sample Nos. Y-20 and Y-21	7
7	Stagnation point ablation as a function of time for sample Nos. Y-22 and Y-23	8
8	Stagnation point ablation as a function of time for sample No. Y-31	8
9	Stagnation point ablation as a function of time for sample Nos. Y-32 and Y-33	8
10	Stagnation point ablation as a function of time for sample Nos. Y-34 and Y-35	8
11	Sample No. Y-1 after testing	12
12	Silhouettes of sample No. Y-1 before and after testing	12
13	Sample No. Y-2 after testing	13
14	Silhouettes of sample No. Y-2 before and after testing	13
15	Sample No. Y-3 after testing	14
16	Silhouettes of sample No. Y-3 before and after testing	14
17	Sample No. Y-4 after testing.	15
18	Sectional view of sample No. Y-4 after testing . .	15
19	Silhouettes of sample No. Y-4 before and after testing	15
20	Sample No. Y-5 after testing.	16
21	Sectional view of sample No. Y-5 after testing . .	16

LIST OF ILLUSTRATIONS (continued)

Figure		Page
22	Silhouettes of sample No. Y-5 before and after testing.	16
23	Silhouettes of sample No. Y-6 before and after testing.	17
24	Silhouettes of sample No. Y-7 before and after testing.	18
25	Sample No. Y-8 after testing	19
26	Sectional view of sample No. Y-8 after testing	19
27	Silhouettes of sample No. Y-8 before and after testing.	19
28	Sample No. Y-9 after testing	20
29	Sample No. Y-10 after testing.	20
30	Sample No. Y-17 after testing.	21
31	Sectional view of sample No. Y-17 after testing	21
32	Silhouettes of sample No. Y-17 before and after testing.	21
33	Sample No. Y-18 after testing.	22
34	Sectional view of sample No. Y-18 after testing	22
35	Silhouettes of sample No. Y-18 before and after testing.	22
36	Sample No. Y-19 after testing.	23
37	Sectional view of sample No. Y-19 after testing	23
38	Silhouettes of sample No. Y-19 before and after testing.	23
39	Sample No. Y-20 after testing.	24
40	Sectional view of sample No. Y-20 after testing	24
41	Silhouettes of sample No. Y-20 before and after testing.	24
42	Sample No. Y-21 after testing.	25
43	Sectional view of sample No. Y-21 after testing	25
44	Silhouettes of sample No. Y-21 before and after testing.	25

LIST OF ILLUSTRATIONS (continued)

Figure		Page
45	Sample No. Y-22 after testing.	26
46	Sectional view of sample No. Y-22 after testing .	26
47	Silhouettes of sample No. Y-22 before and after testing.	26
48	Sample No. Y-23 after testing.	27
49	Sectional view of sample No. Y-23 after testing .	27
50	Silhouettes of sample No. Y-23 before and after testing.	27
51	Sample No. Y-31 after testing.	28
52	Sectional view of sample No. Y-31 after testing .	28
53	Silhouettes of sample No. Y-31 before and after testing.	28
54	Sample No. Y-32 after testing.	29
55	Sectional view of sample No. Y-32 after testing .	29
56	Silhouettes of sample No. Y-32 before and after testing.	29
57	Sample No. Y-33 after testing.	30
58	Sectional view of sample No. Y-33 after testing .	30
59	Silhouettes of sample No. Y-33 before and after testing.	30
60	Sample No. Y-34 after testing.	31
61	Sectional view of sample No. Y-34 after testing .	31
62	Silhouettes of sample No. Y-34 before and after testing.	31
63	Sample No. Y-35 after testing.	32
64	Sectional view of sample No. Y-35 after testing .	32
65	Silhouettes of sample No. Y-35 before and after testing.	32

LIST OF TABLES

Table		Page
1	Sample Identification	4
2	Test Results	5

1. INTRODUCTION

This report is primarily a presentation of test results obtained on a series of twenty-two samples tested under a supplementary agreement of USAF Contract No. AF 33(616)-5436. Additional testing was also carried out under the parent program. The results of these other tests, and a complete report of other activities on the project, are reported in WADC TR 59-87, Part I.

All twenty-two samples reported upon herein were tested at approximately identical heat flux rates in the plasma discharge of an air-stabilized arc. The sample shape, test conditions, and the material behavior are described in the following sections.

2. TEST DESCRIPTION

2.1 OPERATING CONDITIONS AND SAMPLE POSITION

All samples were tested in the CML 1.1-megawatt air-stabilized arc. Test conditions were:

Arc current (amp)	3500
Arc voltage (volts)	300
Mass flow (lb/sec)	0.25
Stagnation heat flux rate (B/ft^2-sec)	1950
Distance of sample nose above top electrode (in.)	4.5
Approximate gas velocity (ft/sec)	2500
Approximate stagnation gas temperature (^oK)	9000
Nominal test duration (sec)	30

2.2 SAMPLE SHAPE

The standard sample shape for all materials tested is shown in Fig. 1. All samples were supplied through WADC.

2.3 TEST PROCEDURE

The sample, attached to the sample holder, was located approximately 22 inches above the cathode and was protected from the plasma jet by a transite shield. After the arc was brought to the operating conditions listed above, the

---

Manuscript released by the author 29 January 1959 for publication as a WADC Technical Report.

sample and the protective shield were lowered until the sample was in the proper position in the jet. At this time, the shield was withdrawn to expose the sample. This sudden exposure yielded a step change in the heat input.

The following information was recorded for all samples: weights before and after testing; duration of test; and over-all dimensional changes as shown by silhouettes made before and after heating. Photographs of the samples after heating were taken to show surface conditions, evidence of cracking, etc. Color motion pictures were taken at 32 frames per second during the testing of each sample, allowing the construction of curves of stagnation point ablation versus time for the test period. In addition to this information pertaining to the sample, the arc operating parameters were recorded to insure reproducibility of test conditions.

2.4 MATERIALS TESTED

A list of the materials tested is given in Table 1, which includes the WADC Code Number and the CML Code Number for the sample, the sample composition, and, for reinforced plastics, the orientation of the reinforcement material. The material identification given in Table 1 is merely a generic classification to denote the general type of material tested; more detailed identification cannot be made since it would involve the use of proprietary information.

3. TEST RESULTS

Table 2 lists the actual test duration; the weights before and after testing; the per cent weight loss; and the stagnation point linear ablation for each sample tested.

The ablated thickness of the material at the stagnation point was obtained from the motion pictures for 15 of the samples and plotted as a function of time in Fig. 2. For the graphite samples Y-1 through Y-3 these curves were not plotted. For these samples the total stagnation point ablation in the test was less than 0.1 inch, and the ablation was almost linear with time. The curves were not plotted for samples Y-4, Y-9, and Y-10, since these samples failed during testing by spalling. During the testing of sample Y-18, the motion picture camera jammed and the information required for plotting the ablation curve was not obtained. For more ease in interpretation of individual test results, the curves shown in Fig. 2 are plotted with fewer curves on each graph in Figs. 3 through 10.

Photographs of the samples and sample cross sections after testing, silhouettes of the samples before and after testing, and remarks concerning material behavior in the individual tests are included in Appendix I.

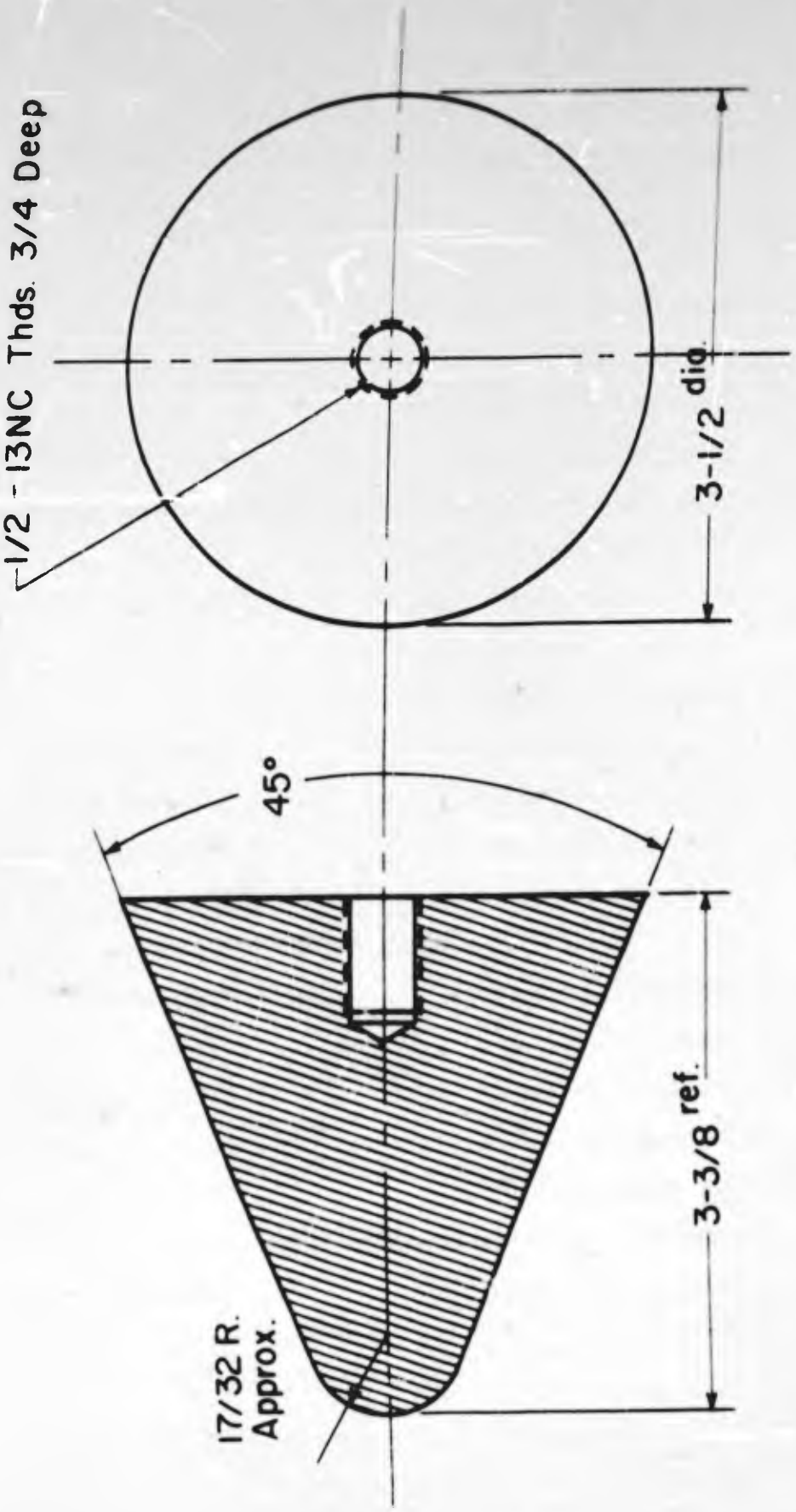

Figure 1. Standard sample shape.

Table I

Sample Identification

Sample No.		Sample Composition	Reinforcement Orientation
CML	WADC		
Y-1	I	ATJ Graphite	
Y-2	II	High Density Graphite	
Y-3	III	Coated ATJ Graphite	
Y-4	IV	Intermetallic Compound	
Y-5	V	Phenylsilane-glass	Fabric parallel to base
Y-6	VI	Phenylsilane-glass	Chopped fabric
Y-7	VII	Phenolic-ceramic fiber	Random
Y-8	VIII	Phenolic-ceramic fiber	Random
Y-9	IX	Graphite, molded	
Y-10	X	Graphite, molded	
Y-17	XI	Phenolic-Refrasil	Chopped fabric
Y-18	XII	Phenolic-Refrasil	Chopped fabric
Y-19	XIII	Phenolic-Refrasil	Fabric parallel to base
Y-20	XIV	Epoxy-ceramic fiber	Random
Y-21	XV	Epoxy-glass fiber-ceramic fiber	Random
Y-22	XVI	Phenolic-asbestos	Random
Y-23	XVII	Phenolic-asbestos	Random
Y-31	XVIII	Phenolic-nylon	Fabric perpendicular to base
Y-32	XIX	Phenolic-nylon	Chopped fabric
Y-33	XX	Melamine-nylon	Chopped fabric
Y-34	XXI	Phenolic-asbestos-graphite	Random
Y-35	XXII	Silicone-asbestos	Random

Table 2

Test Results

Sample No.		Duration of Exposure (sec)	Weight (gm)		Wt. Loss (%)	Stagnation Point Ablation (in.)
CML	WADC		Before	After		
Y-1	I	31.2	384.6	362.3	5.8	0.09
Y-2	II	30.8	387.8	360.9	6.9	0.09
Y-3	III	31.2	385.4	377.0	2.2	0.06
Y-4	IV	35.9*	538.0	493.1	8.3	0.44
Y-5	V	28.1	415.0	299.2	27.9	0.45
Y-6	VI	35.9	391.7	271.2	30.8	0.38
Y-7	VII	32.0	422.2	305.7	27.6	0.38
Y-8	VIII	32.3	380.0	245.7	35.3	0.53
Y-9	IX	4.6	393.3	- - **	- - **	- - **
Y-10	X	3.0	389.8	- - **	- - **	- - **
Y-17	XI	30.3	380.0	303.9	20.0	0.49
Y-18	XII	- - ***	321.6	236.0	26.6	0.51
Y-19	XIII	30.4	389.6	317.2	18.6	0.35
Y-20	XIV	11.9	507.5	126.9	75.0	1.27
Y-21	XV	30.0	472.2	354.0	25.0	0.31
Y-22	XVI	29.9	343.4	230.1	33.0	0.56
Y-23	XVII	30.5	327.1	234.8	28.2	0.36
Y-31	XVIII	28.3	226.1	147.8	34.7	0.20
Y-32	XIX	30.2	265.1	196.6	25.8	0.12
Y-33	XX	28.6	287.2	212.3	26.1	0.27
Y-34	XXI	30.7	384.4	293.5	23.6	0.32
Y-35	XXII	28.2	375.4	259.9	30.8	0.58

* An arc malfunction resulted in two stepwise heatings, of 10- and 26-second durations.

** Both samples started to spall and fly apart almost immediately. Test stopped when samples disappeared.

*** Sixteen-millimeter camera jammed during this test and exact exposure time is unavailable. Probable exposure time between 29- and 31-seconds.

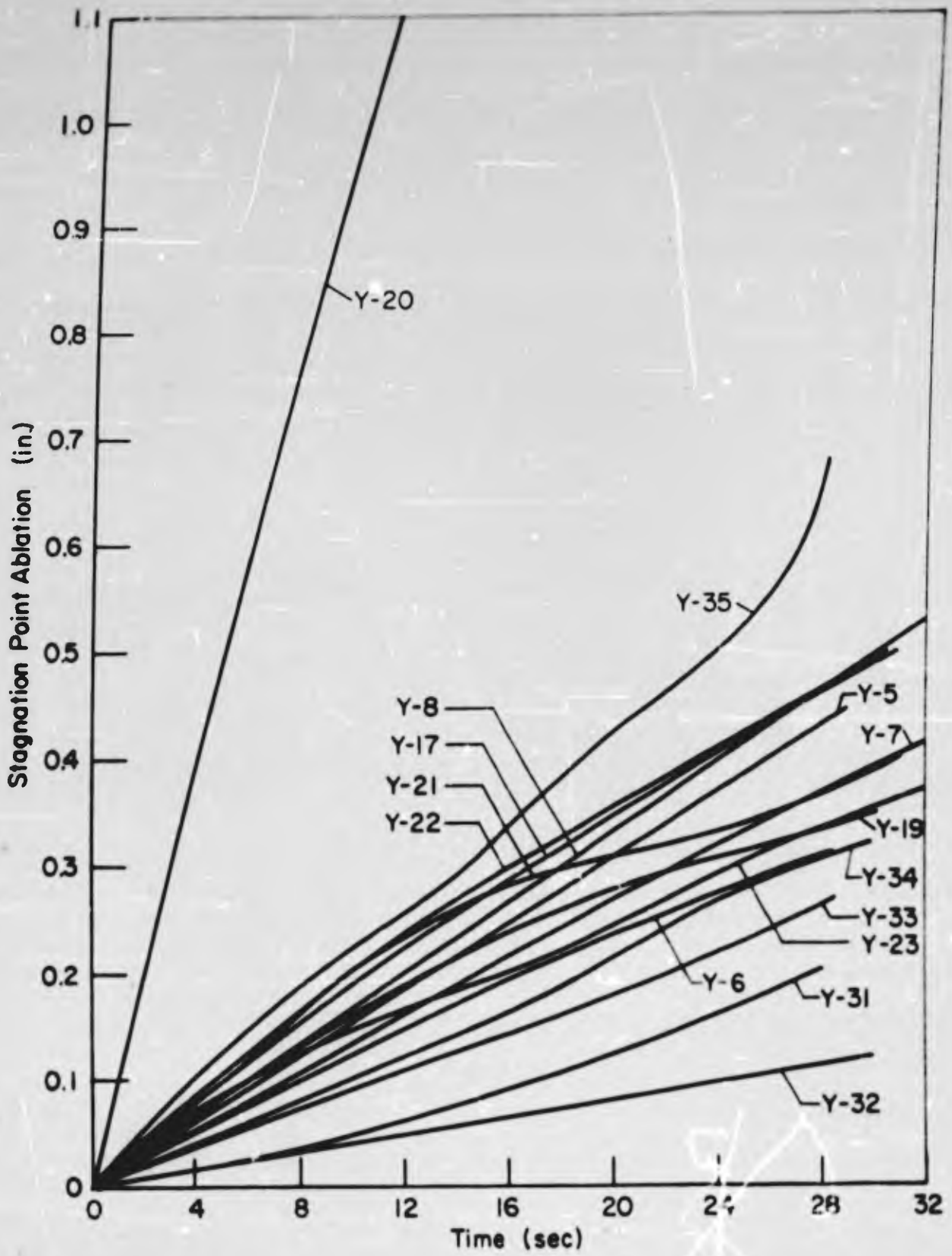

Figure 2. Stagnation point ablation as a function of time for samples as noted.

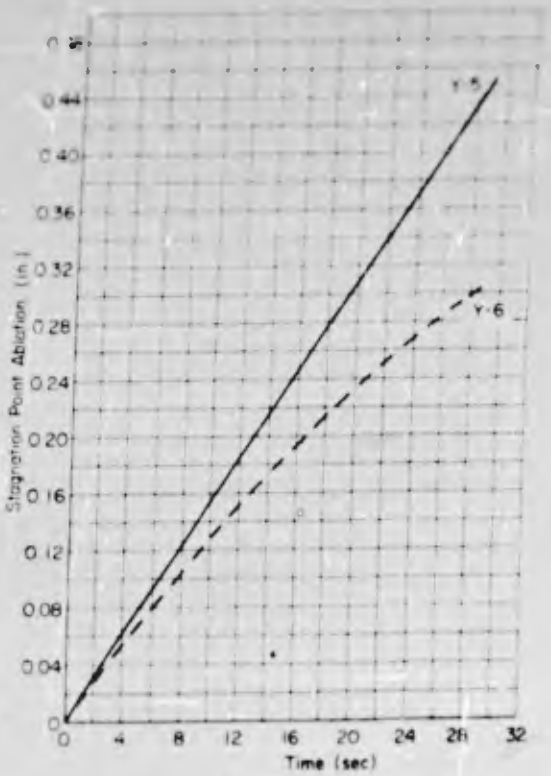

Figure 3. Stagnation point ablation as a function of time for samples Nos. Y-5 and Y-6.

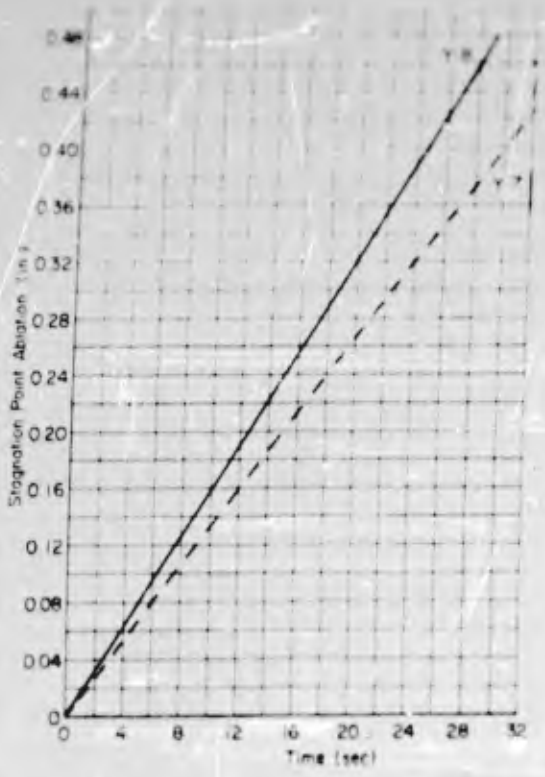

Figure 4. Stagnation point ablation as a function of time for samples Nos. Y-7 and Y-8.

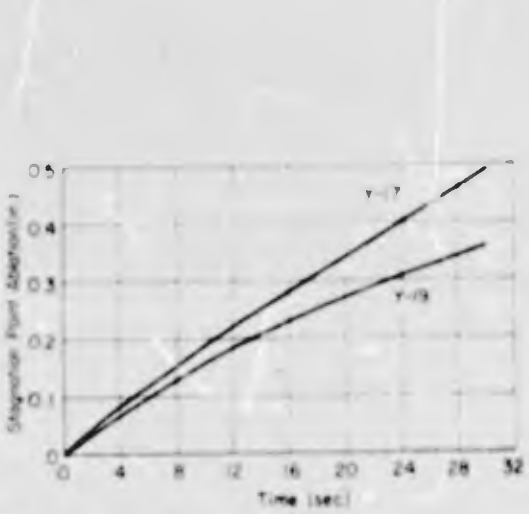

Figure 5. Stagnation point ablation as a function of time for samples Nos. Y-17 and Y-19.

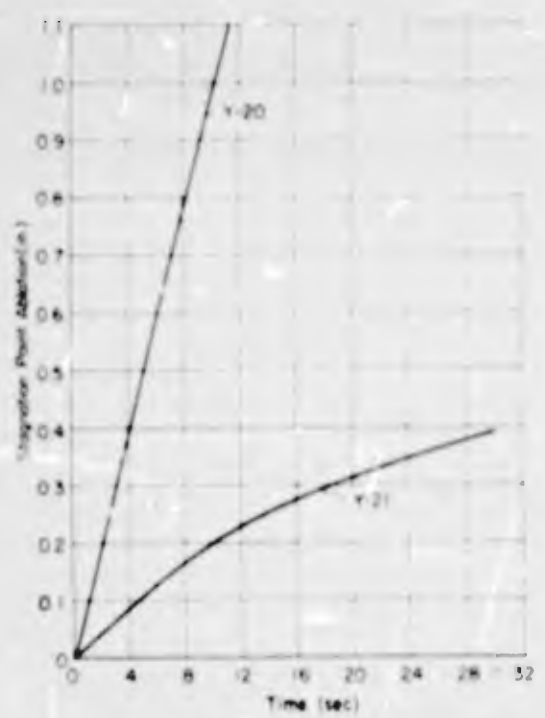

Figure 6. Stagnation point ablation as a function of time for samples Nos. Y-20 and Y-21.

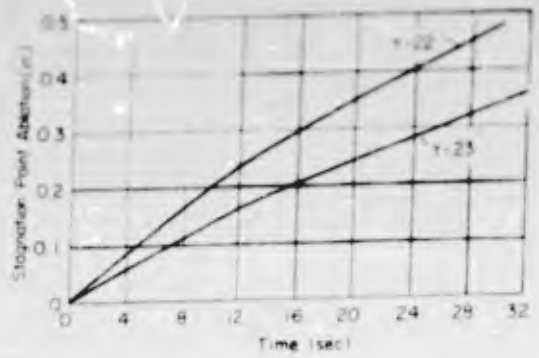

Figure 7. Stagnation point ablation as a function of time for samples Nos. Y-22 and Y-23.

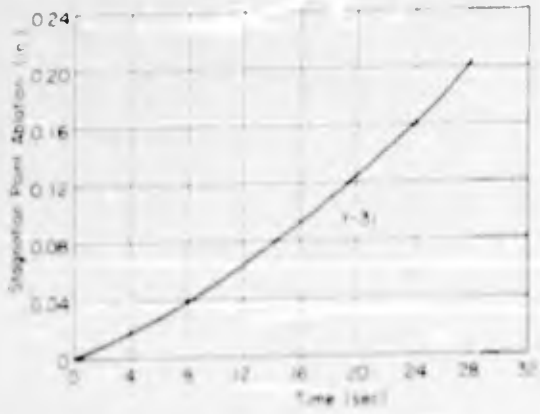

Figure 8. Stagnation point ablation as a function of time for sample No. Y-31.

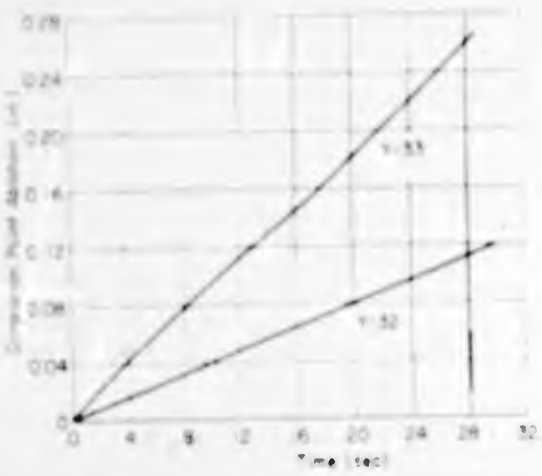

Figure 9. Stagnation point ablation as a function of time for samples Nos. Y-32 and Y-33.

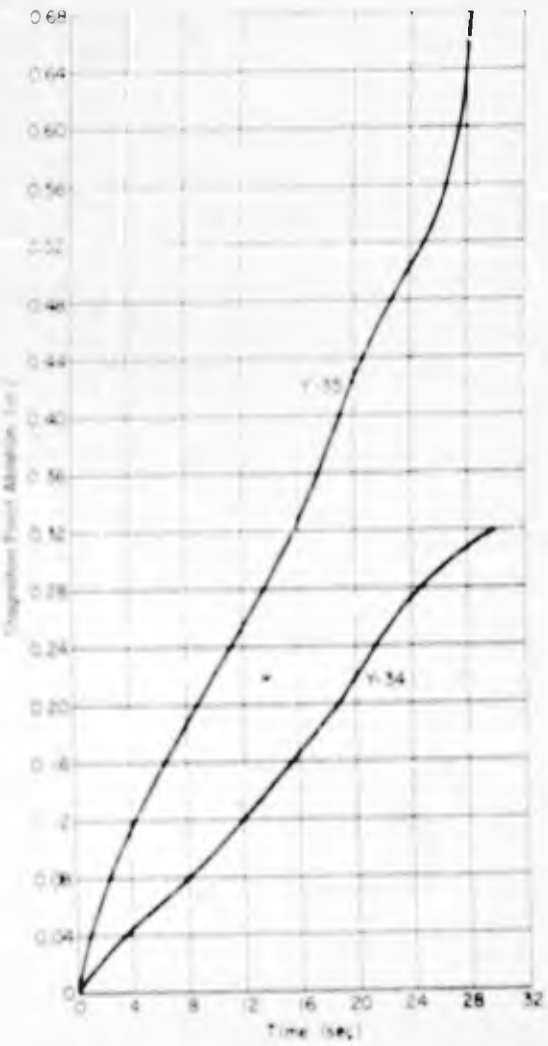

Figure 10. Stagnation point ablation as a function of time for samples Nos. Y-34 and Y-35.

4. GENERAL REMARKS

Based upon examination of the samples after testing and the stagnation point ablation rate data shown in Fig. 2, some general trends of behavior appear. The data are not sufficient to give specific recommendations with regard to such details as orientation of fabric reinforcement on a given material, but when the stagnation point linear ablation rate is used as a performance criterion, the following trends are manifest:

(1) Materials which form only gaseous decomposition products upon heating perform better than materials which form both liquid and gaseous decomposition products. This is apparent from a comparison of the performance of sample Nos. Y-31, Y-32, and Y-33 (gaseous products only) with the performance of sample Nos. Y-5, Y-17, and Y-35 (liquid and gaseous products). The gaseous products evidently achieve better mass transfer cooling action than liquid products.

(2) Materials which form a high emissivity surface upon heating perform better than materials which form a low emissivity surface, because of the ability to reradiate a considerable portion of the heat supplied. This may be seen from a comparison of the performance of sample Nos. Y-31 through Y-33, which formed a black graphitized surface, with the performance of sample Nos. Y-5, Y-8, Y-17, Y-22, and Y-35, which formed a graphitized surface characteristically containing shiny liquid globules of glassy substance.

(3) Materials which form a low density graphite shell upon heating performed very well, as evidenced by the behavior of sample Nos. Y-31 and Y-32. In this connection, it is important to remember that the dynamic pressure in these tests was low. There may be situations in intended applications where the dynamic pressure would be high enough to impose stresses on the graphite shell which would strip it off as it is formed and cause relatively poor ablation performance.

(4) Materials which form a graphite surface upon heating may achieve a performance approaching that obtained with a complete initial composition of graphite, with the advantage that the low thermal conductivity of the unaffected material beneath the surface allows the interior of the sample to remain much cooler than with graphite composition throughout. This could have important applications for back-up structure design.

Appendix I

SAMPLE PHOTOGRAPHS, SILHOUETTES, AND TEST RESULTS

1. INTRODUCTION

This appendix contains:

a. Photographs of the samples taken after testing.

b. Photographs of cross sections of some of the samples after testing.

c. Silhouettes of the samples before and after testing.

d. Remarks concerning individual sample tests. These remarks are based on the evidence of photographs, test observations, and examination of the colored motion pictures.

SAMPLE NO. Y-1

Composition: ATJ Graphite

Remarks: Immediately after the start of heating, some liquid began to flow up the side of the sample. No cracking of the sample was observed.

Figure 11. Sample No. Y-1 after testing.

Figure 12. Silhouettes of sample No. Y-1 before and after testing.

SAMPLE NO. Y-2

Composition: High Density Graphite

Remarks: Immediately after the start of heating, some liquid began to flow up the side of the sample. No cracking of the sample was observed.

Figure 13. Sample No. Y-2 after testing.

Figure 14. Silhouettes of sample No. Y-2 before and after testing.

SAMPLE NO. Y-3

Composition: Coated ATJ Graphite

Remarks: The flow field is slightly asymmetrical although the condition is not serious. Again, liquid is seen leaving the hot nose zone. In addition, there are definite isotherms along the body, corresponding to possible phase changes. No cracking of the sample was observed.

Figure 15. Sample No. Y-3 after testing.

Figure 16. Silhouettes of sample No. Y-3 before and after testing.

SAMPLE NO. Y-4

Composition: Intermetallic Compound

Remarks: Due to a malfunction of the arc, this sample was subjected to two stepwise heatings, of 10- and 26-second durations. Figure 18 shows the depths of penetration of the melted zone at the nose, and also indicates a probable thermal stress failure in the interior. During the early part of the test there was some spalling at the nose.

Figure 17. Sample No. Y-4 after testing.

Figure 18. Sectional view of sample No. Y-4 after testing.

Figure 19. Silhouettes of sample No. Y-4 before and after testing.

SAMPLE NO. Y-5

Composition: Phenylsilane-glass (Fabric parallel to base)

Remarks: During the run, much liquid was stripped away from the surface of the sample. The laminar failure near the base occurred during the latter portion of the test.

Figure 20. Sample No. Y-5 after testing.

Figure 21. Sectional view of sample No. Y-5 after testing.

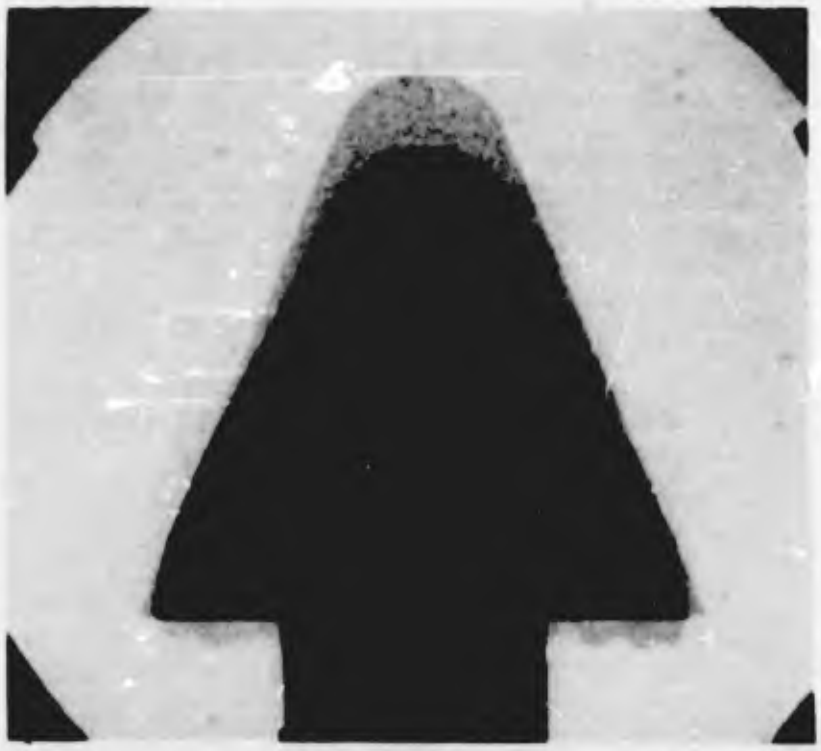

Figure 22. Silhouettes of sample No. Y-5 before and after testing.

SAMPLE NO. Y-6

Composition: Phenylsilane-glass (Chopped fabric)

Remarks: Much spalling occurred over the entire area of the sample during the early part of the test. Later, liquid spilled over the base of the cone. There is definite evidence that the boundary layer in Y-6 is much thicker than in Y-5, which may account for the slower ablation rate.

Sample No. Y-6 was taken away immediately after the test by Mr. Schmidt of WADC, so that no photographs after testing are available.

Figure 23. Silhouettes of sample No. Y-6 before and after testing.

SAMPLE NO. Y-7

Composition: Phenolic-ceramic fiber

Remarks: Some liquid being stripped off and a slight amount of spalling occurred. The surface after test was somewhat roughened.

Sample No. Y-7 was taken away immediately after the test by Mr. Schmidt of WADC, so that no photographs after testing are available.

Figure 24. Silhouettes of sample No. Y-7 before and after testing.

SAMPLE NO. Y-8

Composition: Phenolic-ceramic fiber

Remarks: Again, some liquid left the base of the cone. Little or no spalling occurred, but there was some surface roughening. The boundary layer seems to be fairly thin.

Figure 25. Sample No. Y-8 after testing.

Figure 26. Sectional view of sample No. Y-8 after testing.

Figure 27. Silhouettes of sample No. Y-8 before and after testing.

SAMPLE NOS. Y-9 and Y-10

Composition: Graphite, molded

Remarks: Both samples failed similarly. The shattering of each was almost of an explosive nature, and the pieces were found over an area about 12 by 20 feet, indicating the forceful disintegration. Each test was stopped when the sample had disappeared.

Figure 28. Sample No. Y19 after testing.

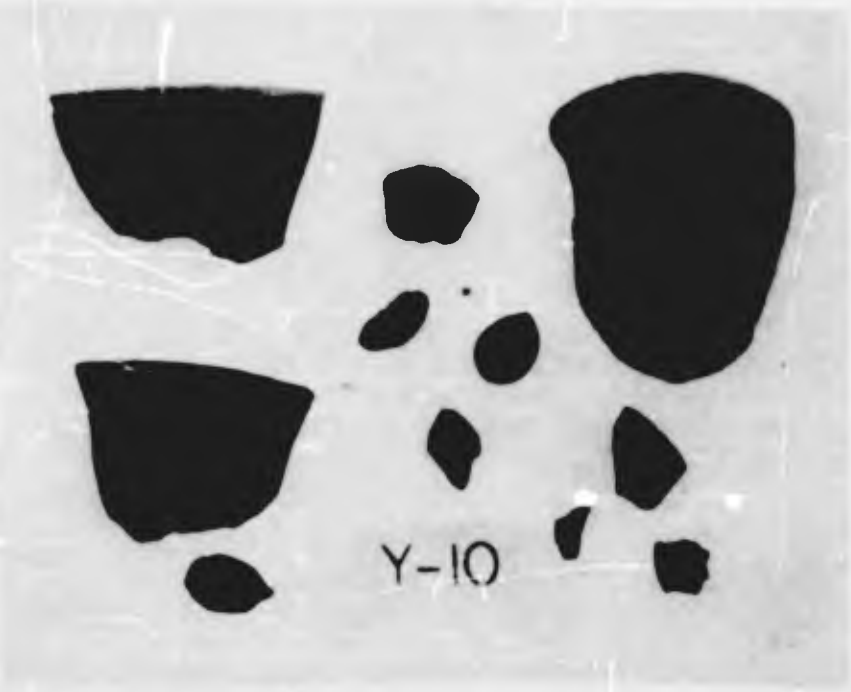

Figure 29. Sample No. Y-10 after testing.

SAMPLE NO. Y-17

Composition: Phenolic-Refrasil (Chopped fabric)

Remarks: The color motion pictures show little liquid leaving the surface of the sample. There is considerable roughening of the surface.

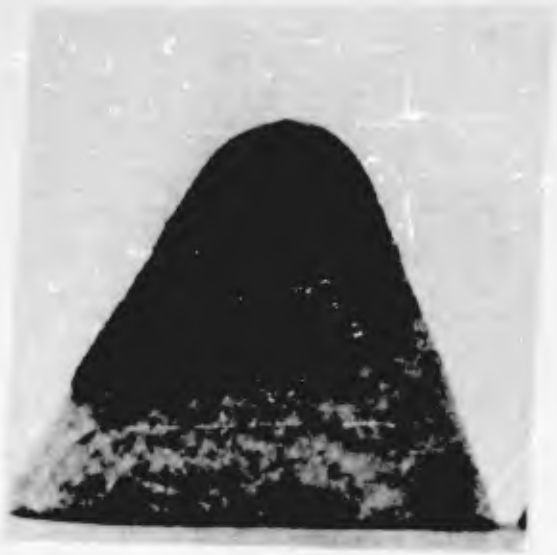

Figure 30. Sample No. Y-17 after testing.

Figure 31. Sectional view of Sample No. Y-17 after testing.

Figure 32. Silhouettes of sample No. Y-17 before and after testing.

SAMPLE NO. Y-18

Composition: Phenolic-Refrasil (Chopped fabric)

Remarks: This sample was identical to Y-17 except for a routed out section to relieve stresses which might cause delamination. It behaved similarly in all respects to Y-17. Neither sample cracked or delaminated. Although the weight loss percentage is somewhat higher, the actual loss of weight is comparable.

Figure 33. Sample No. Y-18 after testing.

Figure 34. Sectional view of sample No. Y-18 after testing.

Figure 35. Silhouettes of sample No. Y-18 before and after testing.

SAMPLE NO. Y-19

Composition: Phenolic-Refrasil (Fabric parallel to base)

Remarks: This sample shows some degree of surface roughening. During the test a small amount of liquid could be seen leaving the base of the cone. This sample was of a laminar structure, but no delamination was noted during testing. However, a delamination was noticed 1-1/8 inches from the stagnation region upon sectioning of the sample, as shown in Fig. 37.

Figure 36. Sample No. Y-19 after testing.

Figure 37. Sectional view of sample No. Y-19 after testing.

Figure 38. Silhouettes of sample No. Y-19 before and after testing.

SAMPLE NO. Y-20

Composition: Epoxy-ceramic Fiber

Remarks: Immediately after the start of heating of the sample thin sheets of material began flying off, and this phenomenon continued during the test. The sample very rapidly lost its hemispherical nose and assumed the pure conical shape illustrated by the after silhouette.

Figure 39. Sample No. Y-20 after testing.

Figure 40. Sectional view of sample No. Y-20 after testing.

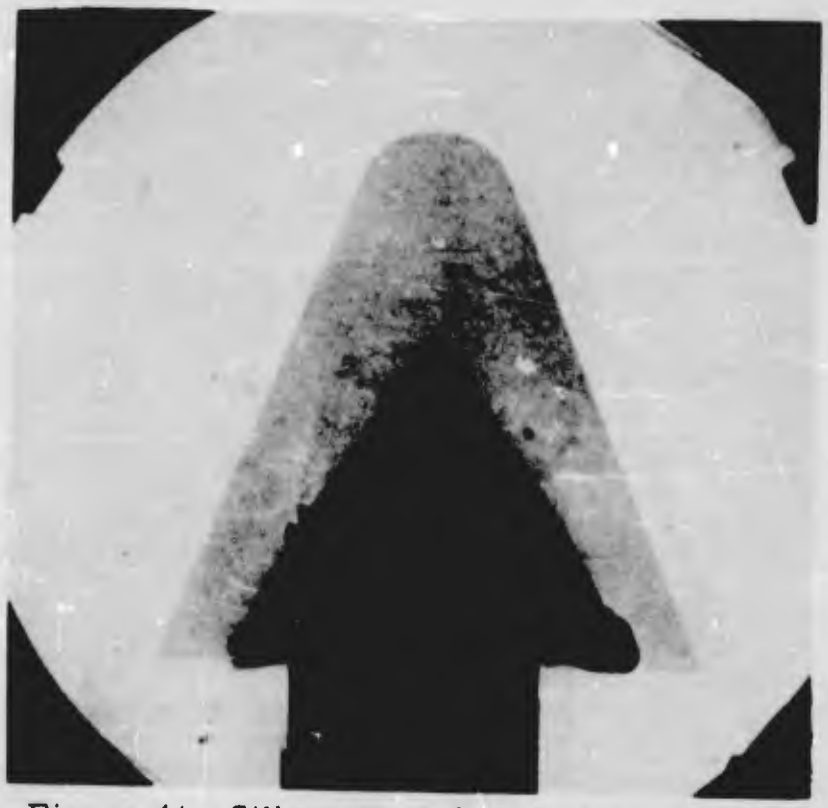

Figure 41. Silhouettes of sample No. Y-20 before and after testing.

SAMPLE NO. Y-21

Composition: Epoxy-glass fiber-ceramic fiber

Remarks: The surface of this sample became pockmarked early in the test. Some liquid was noted leaving the base of the cone, and the surface of the sample was left in a considerably roughened condition after the heating.

Figure 42. Sample No. Y-21 after testing.

Figure 43. Sectional view of sample No. Y-21 after testing.

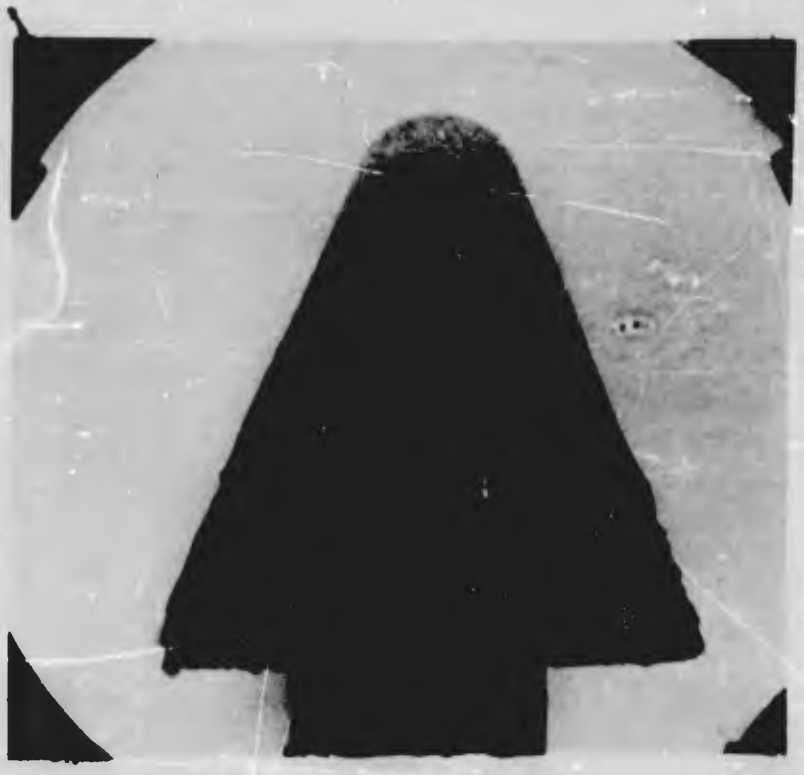

Figure 44. Silhouettes of sample No. Y-21 before and after testing.

SAMPLE NO. Y-22

Composition: Phenolic asbestos

Remarks: A slight amount of pocking was noted early in the heating period, followed by considerable liquid loss from the base of the cone. The surface was left in slightly roughened condition.

Figure 45. Sample No. Y-22 after testing.

Figure 46. Sectional view of sample No. Y-22 after testing.

Figure 47. Silhouettes of sample No. Y-22 before and after testing.

SAMPLE NO. Y-23

Composition: Phenolic-asbestos

Remarks: This sample evidenced much more pocking, as though internal pressures were causing small pieces of the surface to be popped out. Little liquid was lost from the base of the cone, and the surface was left in somewhat better condition than that of the previous sample.

Figure 48. Sample No. Y-23 after testing.

Figure 49. Sectional view of sample No. Y-23 after testing.

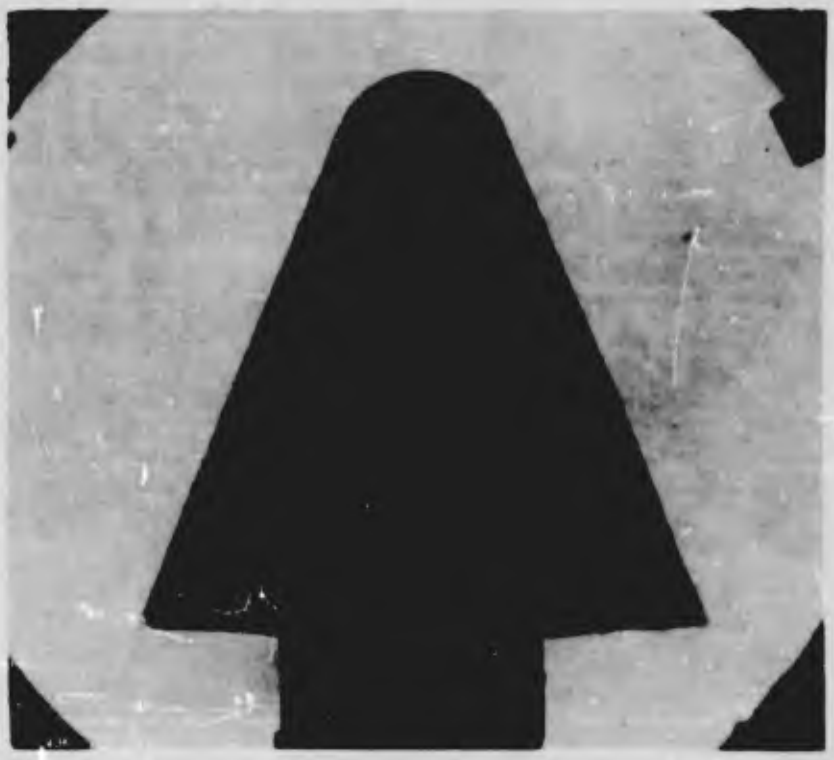

Figure 50. Silhouettes of sample No. Y-23 before and after testing.

SAMPLE NO. Y-31

Composition: Phenolic-nylon (Fabric perpendicular to base)

Remarks: Because this sample was laminated along the axis of the cone, it ablated asymmetrically. This fact is clearly shown in Fig. 51. The motion pictures show a rather thin boundary layer with evidence of surface carbonization and roughening. The heat transferred through the support rod charred the material and made accurate alignment of the silhouette almost impossible. The outer layer came off as a shell during handling for photographic purposes.

Figure 51. Sample No. Y-31 after testing. The view on the right is 90° from that on the left.

Figure 52. Sectional view of sample No. Y-31 after testing.

Figure 53. Silhouettes of sample No. Y-31 before and after testing.

SAMPLE NO. Y-32

Composition: Phenolic-nylon (Chopped fabric)

Remarks: Little information is available from the motion pictures because the film was inadvertently overexposed. The view of the sectioned sample shows that a relatively thin outer shell came loose during handling after the test.

Figure 54. Sample No. Y-32 after testing.

Figure 55. Sectional view of sample No. Y-32 after testing.

Figure 56. Silhouettes of Sample No. Y-32 before and after testing.

SAMPLE NO. Y-33

Composition: Melamine-nylon

Remarks: The motion pictures show no liquid loss from the sample and evidence only a thin boundary layer. The view of the sectioned sample indicates a rather slight heat penetration from the surface.

Figure 57. Sample No. Y-33 after testing.

Figure 58. Sectional view of sample No. Y-33 after testing.

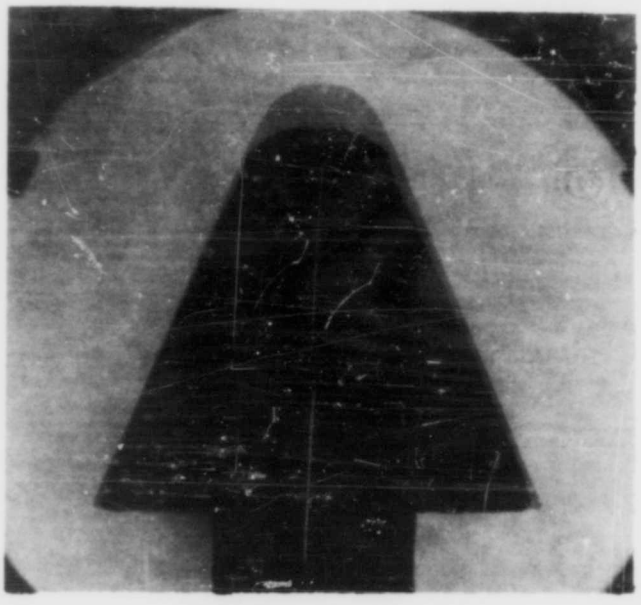

Figure 59. Silhouettes of sample No. Y-33 before and after testing.

SAMPLE NO. Y-34

Composition: Phenolic-asbestos-graphite

Remarks: The motion pictures show some early pocking of the surface and a fairly thick boundary layer. The surface of the sample remained in relatively good condition.

Figure 60. Sample No. Y-34 after testing.

Figure 61. Sectional view of sample No. Y-34 after testing.

Figure 62. Silhouettes of sample No. Y-34 before and after testing.

SAMPLE NO. Y-35

Composition: Silicone-asbestos

Remarks: The motion pictures show that some liquid was lost from the base of the cone and a relatively thin boundary layer. The surface shows considerable roughening.

Figure 63. Sample No. Y-35 after testing.

Figure 64. Sectional view of sample No. Y-35 after testing.

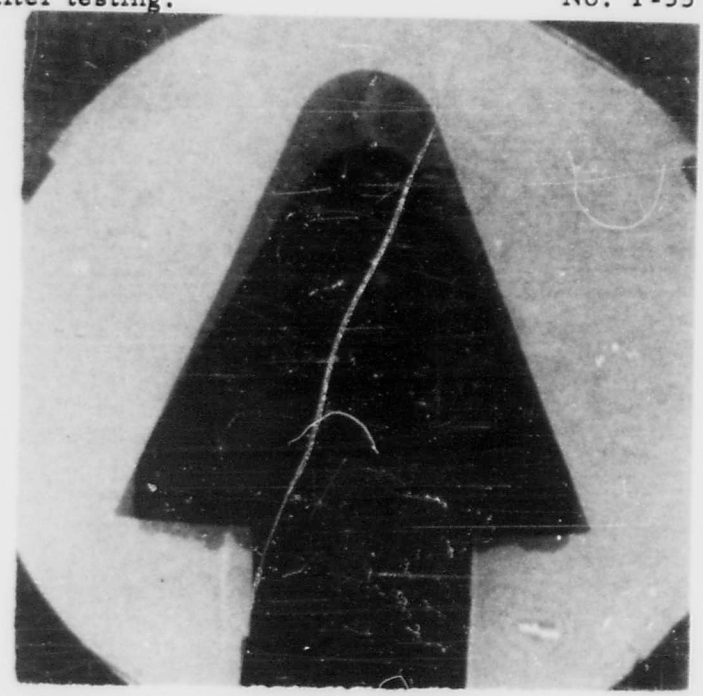

Figure 65. Silhouettes of Sample No. Y-35 before and after testing.

AD

226 368

FOR
MICRO-CARD
CONTROL ONLY

1 OF 1